PHASE EQUILIBRIA AND THERMODYNAMICS OF BINARY COPPER SYSTEMS WITH 3*d*-METALS. VI. COPPER–NICKEL SYSTEM

M. A. Turchanin, P. G. Agraval, and A. R. Abdulov

Thermodynamic evaluation of the Cu–Ni system within the CALPHAD approach is based on values of mixing enthalpies and activities of components in liquid and solid solutions, as well as parameters of phase transformations. The excess Gibbs free energy of phases is described by the following equations: $\Delta G^{L, ex} = x_{Ni}(1 - x_{Ni})(14259 + 0.45T)$ J/mole for liquid alloy and $\Delta G^{(Cu, Ni), ex} = x_{Ni}(1 - x_{Ni}) \times$ $\times (6877.12 + 4.6T + (1 - 2x_{Ni})(-2450.1 + 1.87T))$ J/mole for fcc solution. For the Gibbs free energy of the (Cu, Ni) phase, the magnetic effect is described by the Hillert–Jarl method. The thermodynamic model of the system generates a self-consistent description of all thermodynamic values and phase equilibria. The calculated binodale of fcc solid solution is in satisfactory agreement with experimental data. The critical point have coordinates 605 K and $x_{Ni} = 0.6$.

Keywords: *phase diagram, thermodynamics, thermodynamic modeling, copper-based alloys*

Binary copper–nickel alloys and more complex composites based on them have important mechanical and electrical properties and demonstrate high corrosion resistance in different environments. That is why they are widely used in contemporary industry as structural and electrotechnical materials. Therefore, studying the interaction of copper and nickel is an important task. Processes for extracting these valuable metals from secondary raw materials are another significant application. In this regard, the phase diagram of the system and thermodynamic properties of its phases attracted the close attention of experimenters and were repeatedly subjected to thermodynamic modeling. However, the published data on thermodynamic mixing functions demonstrate substantial differences both in the absolute value and temperature dependence, and phase equilibria in the low-temperature region cannot be considered fully understood.

PHASE EQUILIBRIA IN THE SYSTEM

The system components show complete liquid and solid miscibility. Hence, there are two phases in equilibrium: liquid L and fcc solution (Cu, Ni). The existence of the solid solution was confirmed with optical microscopy and x-ray examination. The solidus and liquidus lines form a cigar-shaped phase diagram with a narrow two-phase region. Different research teams invariably arrived at similar conclusions. The results of research efforts up to 1958 were analyzed in [1].

Contemporary studies of the phase equilibria in the system [2–5] focus of the positioning of the liquidus and solidus lines (Figs. 1 and 2). The papers [2, 3, 5] used for this purpose an x-ray spectral microanalysis of samples quenched from the two-phase region. In addition, the paper [3] established the position of the liquidus line with a thermal analysis followed by extrapolating the data to the zero cooling rate. The measurements made in [3] cover the entire concentration range, the data from [2] the region of copper-rich alloys, and the data from [5] alloys with $x_{Ni} < 0.30$ and $x_{Ni} > 0.70$. The paper [4] studies the phase equilibrium between the liquid and solid solutions with a thermal analysis of seven alloy compositions in the range $x_{Ni} = 0.01–0.87$.
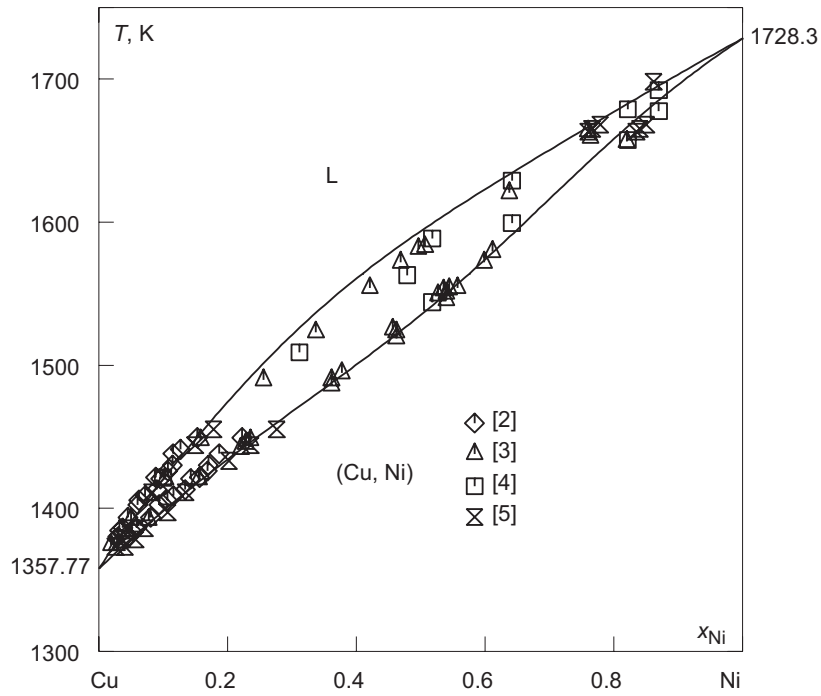

Fig. 1. Experimental and calculated liquidus and solidus lines of the (Cu, Ni) phase: here and below the calculated data are shown as solid lines
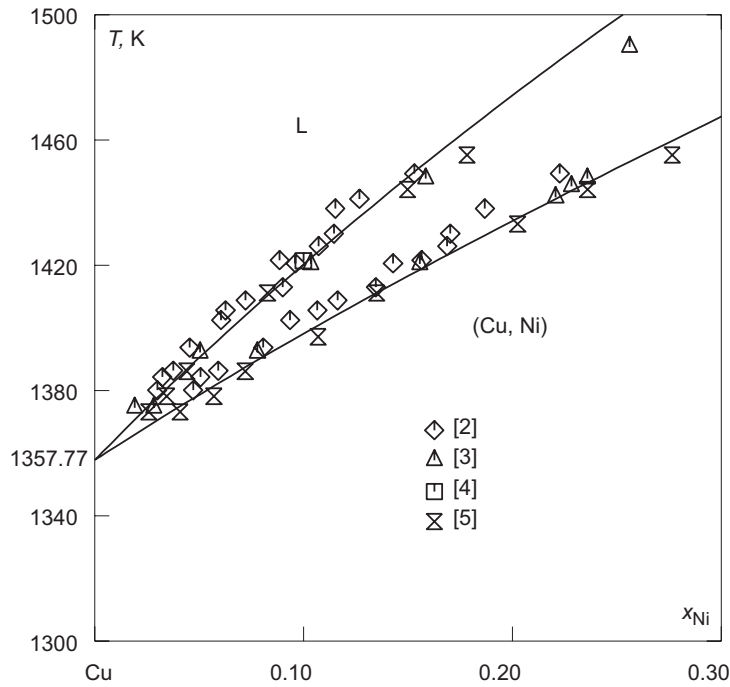

Fig. 2. Liquidus and solidus of the (Cu, Ni) phase for copper-rich alloys

The results obtained in [2–5] are in good agreement. In a wide composition range, the solidus line plotted in these papers is about 30 K higher than that from [1]. According to [3], this difference demonstrates the potential error in determining the solidus temperature when a thermal analysis is the only research method.

As noted above, intermetallides are not formed in the system. The attempts to synthesize CuNi and $CuNi_3$ under high pressures failed [6].
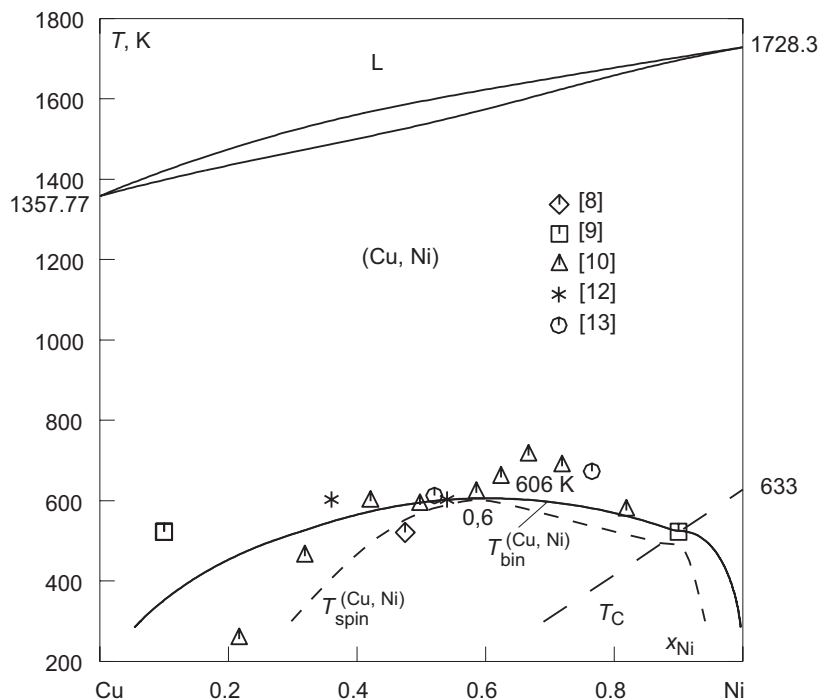
Fig. 3. Copper–nickel phase diagram including the miscibility gap of the (Cu, Ni) phase: the dashed line denotes the boundary of magnetic transformation

The immiscibility of the (Cu, Ni) phase is a serious issue of phase equilibria in the system. The papers devoted to this issue up to 1978 are reviewed in [7]. The studies of electric, magnetic, and structural properties of alloys and their low-temperature thermal capacity show that immiscibility is possible. At the same time, conventional metallographic methods still have not provided direct experimental evidence of immiscibility. Of special attention are the results of the papers [8–12], which examined this phenomenon with highly sensitive diffraction methods.

The paper [8] employs the neutron diffraction method over a range between 298 and 1294 K to examine the short-range order of the Cu–Ni alloy with $x_{Ni} = 0.475$. The results were used to assess the critical miscibility gap temperature, which was 506 to 536 K (Fig. 3). The study [9] carried out an x-ray analysis of the Cu–Ni alloys with different thermal histories and established the immiscibility of solid alloys at 523 K over the concentration range $x_{Ni} = 0.10$–0.90. The thermal neutron diffraction method is employed in [10] to study the short-range order in the hard Cu–Ni alloys. The studies covered compositions $x_{Ni} = 0.1$–0.9 and temperatures 613–973 K. Figure 3 shows the miscibility gap boundaries for hard alloys assessed in [10].

The paper [11] deals with neutron diffraction study of the Cu–Ni alloy with $x_{Ni} = 0.585$ produced from copper and nickel enriched with isotopes. The alloy samples were thermally treated and bombarded with electrons at 373 to 510 K. Based on experimental data on small-angle neutron scattering, the paper [11] established that the composition fluctuated. This was interpreted as evidence of the immiscibility process in hard alloys of the system. The study [12] reports on x-ray structural examination of the alloy with $x_{Ni} = 0.45$ produced by vapor deposition and annealed at 598, 603, and 723 K. Spinodal decomposition of the hard alloy over the range $x_{Ni} = 0.36$–0.54 was revealed at 603 K.

The results of [13] are another evidence of a potential transformation in the (Cu, Ni) phase. There are small jumps, which may be associated with solid immiscibility, on the temperature curves of specific thermal capacity of the alloys with $x_{Ni} = 0.52$ and $x_{Ni} = 0.77$. The points calculated in [13] and indicating the miscibility gap boundaries are shown in Fig. 3 and agree well with other data.

Summarizing the above studies and the papers reviewed in [7], note the following. The immiscibility in the (Cu, Ni) phase may occur in microscopic regions and, therefore, it can hardly be recorded by the conventional metallographic
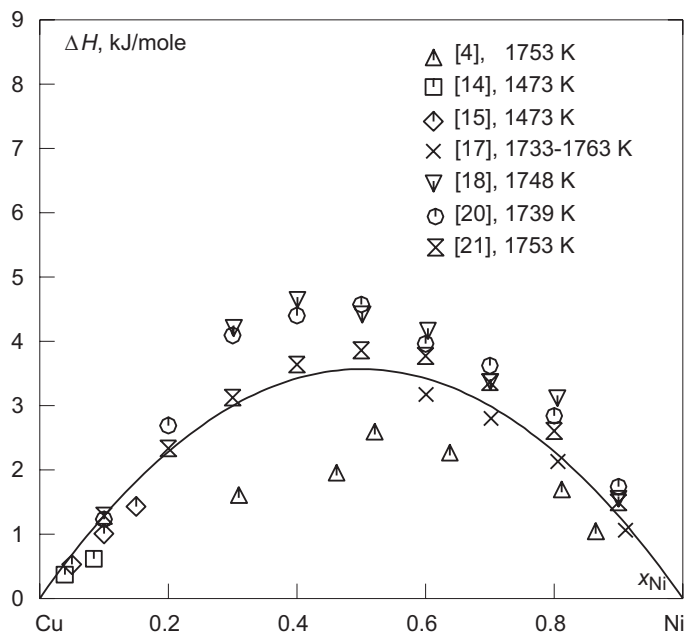
469

Fig. 4. Mixing enthalpy of liquid alloys

method. The critical immiscibility point may be shifted toward the regions of nickel-rich alloys. The last conclusion was further considered in a thermodynamic assessment of the system.

THERMODYNAMIC PROPERTIES OF LIQUID ALLOYS

Mixing Enthalpies. The mixing enthalpies of copper and nickel in liquid alloys were examined with calorimetric methods in [4, 14–21]. The mixing enthalpy of components was first studied in copper-rich melts: in [14] at $x_{Ni} = 0$–0.09 and 1473 K, in [15] at 1473 K and $x_{Ni} = 0$–0.15. Figure 4 presents the results of this study. The paper [16] examined the mixing enthalpy of copper and nickel at 1728 K at $x_{Ni} = 0.158$–0.860. According to [16], the minimum integral mixing enthalpy $\Delta H_{max} = -8.03$ kJ/mole corresponds to an alloy with $x_{Ni} = 0.30$.

The values of integral mixing enthalpy result from measuring thermal effects in the mixing of liquid nickel and copper at 1753 K in [4], at 1739–1763 K in [17], and at 1748 K in [18] for alloys with $x_{Ni} = 0.103$–0.900. According to [17], the maximum ΔH_{max} is 4.4 kJ/mole at $x_{Ni} = 0.45$ (Fig. 4).

The paper [19] examined the partial enthalpy of nickel dissolution in molten copper at 1385 K for alloys with $x_{Ni} \leq 0.03$ and established the first mixing enthalpy of molten supercooled nickel to be $\Delta \overline{H}_{Ni}^{\infty} = 5.4 \pm 0.4$ kJ/mole.

Integral mixing enthalpy was determined for four alloys with $x_{Ni} = 0.601$–0.911 at 1739 K in [20]. The results are presented in Fig. 4.

The partial mixing enthalpies of components are examined in [21] at 1753 K. The concentration dependence of the partial mixing enthalpy of nickel is studied in four independent experiments at $x_{Ni} = 0$–0.48, and the partial mixing enthalpy of copper in three experiments at $x_{Ni} = 0.46$–1. The first mixing enthalpy of nickel and copper was $\Delta \overline{H}_{Ni}^{\infty} = 14.0 \pm 4.0$ kJ/mole. The paper [21] also reports on the first mixing enthalpy of copper and nickel: $\Delta \overline{H}_{Cu}^{\infty} = 16.8 \pm 4.5$ kJ/mole. The following expressions are valid for the concentration dependence of the integral and partial mixing enthalpies of system components:

$$\Delta H = x_{Ni} (1 - x_{Ni}) (14.02 + 2.83 \, x_{Ni}) \text{ kJ/mole},$$

$$\Delta \overline{H}_{Ni} = (1 - x_{Ni})^2 (14.02 + 5.66 \, x_{Ni}) \text{ kJ/mole},$$

$$\Delta \overline{H}_{Cu} = x_{Ni}^2 (11.19 + 5.66 \, x_{Ni}) \text{ kJ/mole}.$$
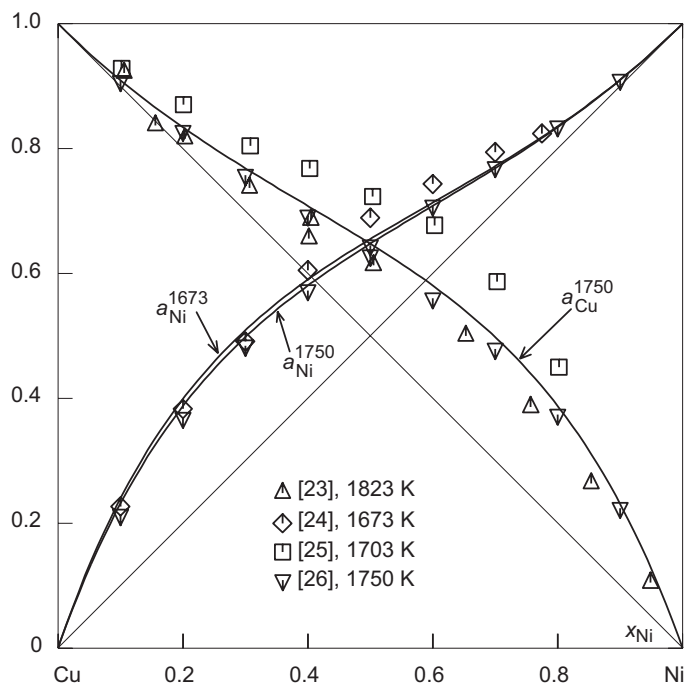
Fig. 5. Thermodynamic activities of liquid alloy components

According to [21], integral mixing enthalpy is a positive value (Fig. 4); its maximum reaches $\Delta H_{max} = 3.9 \pm 0.6$ kJ/mole near the equiatomic composition.

Figure 4 shows that the integral mixing enthalpies of copper and nickel assessed in [17, 18, 20, 21] agree well. The ΔH values reported in [4] are less endothermic. The results of [16] should be critically addressed as the ΔH sign contradicts other data.

The positive values of the integral mixing enthalpy are also evidenced by the paper [22], which examined the high-temperature enthalpy constituent of molten copper, nickel, and four alloys with $x_{Ni} = 0.21–0.81$ at 1873 K. The paper established that the high-temperature enthalpy constituent of molten alloys was somewhat higher than the additive value based on this property of pure components.

Thermodynamic Activities of Melt Components. The thermodynamic activities of components were examined in [23–25]. The paper [23] studied the partial copper pressure with a carrying gas method at 1873 K. These data were used to calculate copper activities (Fig. 5). They indicate insignificant positive deviations of the thermodynamic properties from ideal behavior. The emf method with a solid electrolyte at 1673 K was employed in [24] to examine the thermodynamic activity of nickel. The resulting properties are presented in Fig. 5. The Knudsen effusion method of measuring vapor pressure was used in [25] to study the thermodynamic activities of copper at 1703 K. The results are presented in Fig. 5. The study covered the melts with $x_{Ni} = 0.1018–0.8017$. The results sufficiently agree with [23, 24] but are indicative of greater positive deviations from ideal behavior.

The excessive thermodynamic properties of the melts were examined with Knudsen-cell mass spectrometry in [26]. Based on the vapor composition over the alloys with $x_{Ni} = 0.0754–0.8588$ at $T = 1750$ K, the following expression was derived for the excess free mixing energy:

$$\Delta G^{ex} = x_{Ni}(1 - x_{Ni})(11589 + 1.409T + (1789 - 0.593T)(2x_{Ni} - 1)) \text{ J/mole.}$$

According to this work, the maximum excess free mixing energy reaches $\Delta G_{max}^{ex} = 3.515$ kJ/mole at $x_{Ni} = 0.514$ and maximum integral mixing enthalpy is $\Delta H_{max} = 2.915$ kJ/mole at $x_{Ni} = 0.538$. Figure 5 shows the thermodynamic activities of the components at $T = 1750$ K calculated using the above expression.
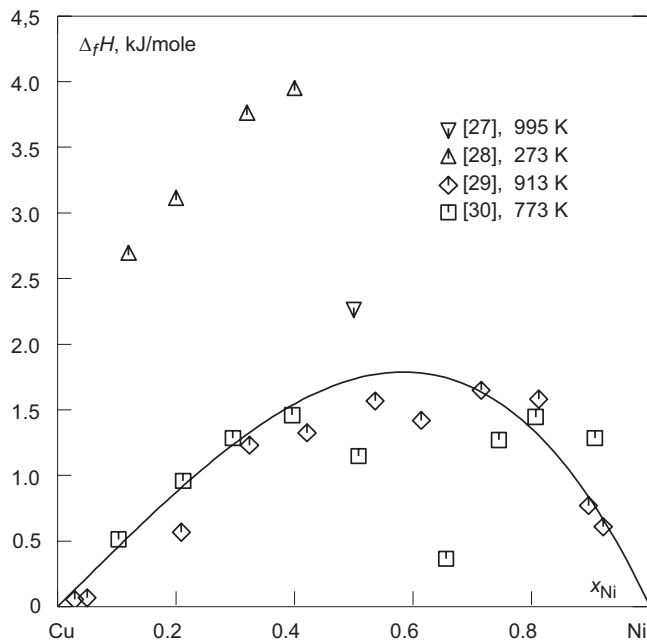
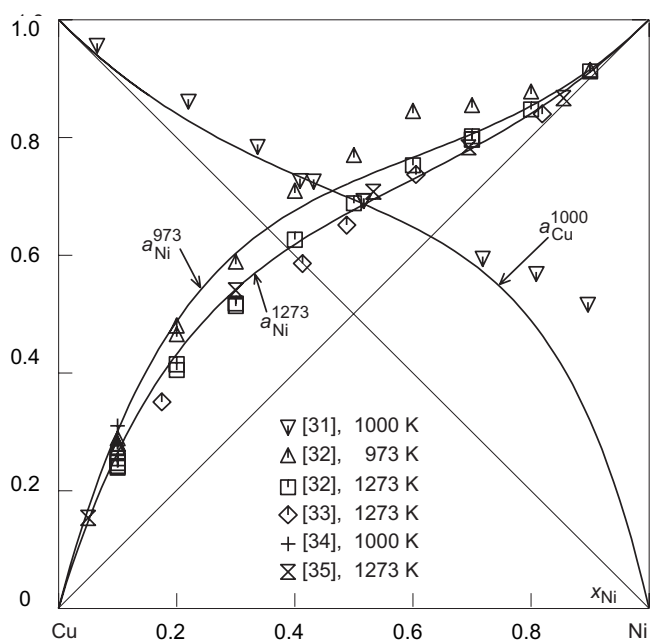*Fig. 6.* Mixing enthalpy of the (Cu, Ni) phase

Fig. 7. Thermodynamic activities of (Cu, Ni) phase components

These data show that the thermodynamic properties of the Cu–Ni melts have positive deviations from ideal behavior. The excessive thermodynamic properties of the melts reach their maximums near the equiatomic composition. There are no experimental data that would directly or indirectly indicate that the excessive thermal capacity of the melts is different from zero.

THERMODYNAMIC PROPERTIES OF HARD ALLOYS

Mixing Enthalpy of Solid Solution. The paper [27] used a calorimetric method to determine the mixing enthalpy in the equiatomic alloy at 995 K (Fig. 6). The papers [28, 29] examined the mixing enthalpies of solid solution components with calorimetric dissolution in liquid tin. The dissolution heat of Cu–Ni alloys is studied in [28] at 623 K. The data from [28] were recalculated into the mixing enthalpy at 273 K (Fig. 6). The mixing enthalpies at 913 K (Fig. 6) are reported in [29]. Using a high-temperature adiabatic calorimeter, the paper [30] examined the mixing enthalpies of hard Cu–Ni alloys at 773 K and the heat capacity of the alloy with $x_{Ni} = 0.7$ at 773 to 1273 K. The ΔH values assessed in [30] are presented in Fig. 6.

The paper [13] used an adiabatic calorimeter to study the specific heat capacity of pure, copper, nickel, and three Cu–Ni alloys between 308 and 883 K. These data were used to calculate the excessive heat capacity of hard alloys at $T = 883$ K, which hence is no more than 0.5 J/(mole · K).

Thermodynamic Activities of Solid Solution Components. The thermodynamic activity of copper in a solid solution was examined with the emf method with a liquid salt electrolyte at 1000 K [31]. The resulting isotherm a_{Cu} is shown in Fig. 7.

The thermodynamic properties of the (Cu, Ni) phase were examined with the emf method with a solid oxide electrolyte [32–34]. The paper [32] studied the thermodynamic activity of nickel at 973 and 1273 K for the alloys with $x_{Ni} = 0.1$–0.9; the isotherms a_{Ni} at these temperatures (Fig. 7) were obtained as a result. Thermodynamic properties are examined between 1173 and 1373 K in [33]; the isotherm a_{Ni} is obtained at 1273 K as a result (Fig. 7). The paper [34] used the emf method with a solid oxide electrolyte to determine the thermodynamic activity of fcc nickel ($a_{Ni} = 0.31$) in a hard alloy with $x_{Ni} = 0.1$ at 1000 K.

The paper [35] employed the thermal emf method to study the thermodynamic properties of the alloys between 1173 and 1373 K. The resulting isotherm a_{Ni} at 1273 K is provided in Fig. 7.

Figure 6 shows that the hard alloys of the system have positive integral mixing enthalpies. The data of all the papers agree well. The only exception is [28], whose results demonstrate high endothermicity. The results of [29, 30] demonstrate that the maximum of this function may be shifted toward nickel-rich alloys. Similar conclusions were made in [31, 36, 37], which determined integral mixing enthalpy by indirect methods. Given small ΔH absolute values and experimental data scattered among different papers, it is difficult to conclude on a temperature dependence of this property.

The thermodynamic activities of hard alloy components also show positive deviations from ideal behavior. The isotherms a_{Ni} obtained in [32, 33, 35] at 1273 K agree well. According to [32], the thermodynamic activity of nickel decreases with increasing temperature.

The nature of interactions in the (Cu, Ni) phase is evidence of its possible immiscibility at low temperatures. The maximum ΔH is shifted toward nickel-rich alloys; this agrees with the possible displacement of the critical immiscibility point to this concentration region, as noted in the first section.

THERMODYNAMIC MODELS AND OPTIMIZATION OF THE SYSTEM

The phase equilibria in the copper–nickel system were repeatedly subjected to thermodynamic modeling. However, there are only few studies [7, 38–40] where such calculations were carried out based on consistent data on the thermodynamic properties of phases and phase boundaries. The calculations performed in [38, 39] do not take into account the magnetic contribution to the free energy of the (Cu, Ni) phase. The paper [40] considers the magnetic contribution using the technique [41, 42]. The thermodynamic description of the system in [7] is based on adding the magnetic contribution to the model [39]. All the above papers reached fundamental agreement between the calculated and experimental values, but none is based on full data on the thermodynamic properties of the phases, especially those related to system melts.

Self-consistent thermodynamic parameters for copper–nickel phases, which correspond to the thermodynamic properties and phase transformations, are calculated in this paper using the CALPHAD approach [43].

Liquid Solution. The temperature and concentration dependence of the Gibbs free energy of liquid alloys was described as follows:

$$G^{\text{L}} = (1 - x_{\text{Ni}})(^{\circ}G_{\text{Cu}}^{\text{L}} - H_{\text{Cu}}^{\text{SER}}) + x_{\text{Ni}}(^{\circ}G_{\text{Ni}}^{\text{L}} - H_{\text{Ni}}^{\text{SER}}) + RT((1 - x_{\text{Ni}})\ln(1 - x_{\text{Ni}}) + x_{\text{Ni}} \ln x_{\text{Ni}}) + \Delta G^{\text{L, ex}}(x_{\text{Ni}}, T),$$

where $(^{\circ}G_{\text{Ni}}^{\text{L}} - H_{\text{Ni}}^{\text{SER}})$ and $(^{\circ}G_{\text{Cu}}^{\text{L}} - H_{\text{Cu}}^{\text{SER}})$ are the Gibbs energies of pure liquid nickel and copper; $\Delta G^{\text{L, ex}}(x_{\text{Ni}}, T)$ is the excess constituent of the Gibbs free energy. The temperature and concentration dependence of the excess Gibbs free energy is as follows

$$\Delta G^{\text{L, ex}} = (1 - x_{\text{Ni}})x_{\text{Ni}} \sum_{i=0}^{n} (1 - 2x_{\text{Ni}})^{i} (A_i + B_i T),$$

where A_i, B_i are coefficients of the model; i is the power of the Redlich–Kister polynomial.

Solid Solution. The temperature and concentration dependence of Gibbs free energy of the (Cu, Ni) phase was described as follows:

$$G^{(\text{Cu, Ni})} = (1 - x_{\text{Ni}})(^{\circ}G_{\text{Cu}}^{(\text{Cu, Ni})} - H_{\text{Cu}}^{\text{SER}}) + x_{\text{Ni}}(^{\circ}G_{\text{Ni}}^{(\text{Cu, Ni})} - H_{\text{Ni}}^{\text{SER}}) +$$

$$+ RT((1 - x_{\text{Ni}})\ln(1 - x_{\text{Ni}}) + x_{\text{Ni}} \ln x_{\text{Ni}}) + \Delta G^{(\text{Cu, Ni), ex}}(x_{\text{Ni}}, T) + \Delta G_{\text{magn}}^{(\text{Cu, Ni})}(x_{\text{Ni}}, T),$$

where $(^{\circ}G_{\text{Cu}}^{(\text{Cu, Ni})} - H_{\text{Cu}}^{\text{SER}})$ and $(^{\circ}G_{\text{Ni}}^{(\text{Cu, Ni})} - H_{\text{Ni}}^{\text{SER}})$ are the Gibbs energies of pure copper and nickel with a fcc structure, $\Delta G^{(\text{Cu, Ni), ex}}(x_{\text{Ni}}, T)$ is the excess constituent of the free energy; $\Delta G_{\text{magn}}^{(\text{Cu, Ni})}(x_{\text{Ni}}, T)$ is the magnetic contribution to the Gibbs energy of the alloy. The excess constituent of the Gibbs free energy of the solid solution was

described by the expression similar to that for the liquid alloy. To model the magnetic contribution to the free energy of fcc solid solutions, the technique proposed in [41, 42] was used:

$$\Delta G_{\text{magn}}^{(\text{Cu, Ni})}(x_{\text{Ni}}, T) = RT(\ln\beta^{(\text{Cu, Ni})} + 1)f(\tau),$$

where $\tau = T / T_C^{(\text{Cu, Ni})}$, $T_C^{(\text{Cu, Ni})}$ is the Curie temperature of the alloy; $\beta^{(\text{Cu, Ni})}$ is the mean magnetic moment of the alloy per atom. The function $f(\tau)$ is defined by

$$f(\tau) = 1 - \frac{1}{D}\left[\frac{79}{140 \cdot p \cdot \tau} + \frac{474}{497}\left(\frac{1}{p} - 1\right)\left(\frac{\tau^3}{6} + \frac{\tau^9}{135} + \frac{\tau^{15}}{600}\right)\right], \tau \leq 1,$$

$$f(\tau) = -\frac{1}{D}\left[\frac{\tau^{-5}}{10} + \frac{\tau^{-15}}{315} + \frac{\tau^{-25}}{1500}\right], \tau > 1,$$

where $D = \dfrac{518}{1125} + \dfrac{11692}{15975}\left(\dfrac{1}{p} - 1\right)$. For an fcc lattice, $p = 0.28$. The concentration dependence of the Curie temperature $T_C^{(\text{Cu, Ni})}$ and mean magnetic moment $\beta^{(\text{Cu, Ni})}$ in the alloy was described as follows:

$$T_C^{(\text{Cu, Ni})} = x_{\text{Ni}}\,{}^\circ T_{C_{\text{Ni}}} + (1 - x_{\text{Ni}})x_{\text{Ni}}\sum_{i=0}^{n}(1 - 2x_{\text{Ni}})^i T_{C_{\text{Cu-Ni}}}^{(\text{Cu, Ni}), i},$$

$$\beta^{(\text{Cu, Ni})} = x_{\text{Ni}}\,{}^\circ\beta_{\text{Ni}} + (1 - x_{\text{Ni}})x_{\text{Ni}}\sum_{i=0}^{n}(1 - 2x_{\text{Ni}})^i\beta_{\text{Cu-Ni}}^{(\text{Cu, Ni}), i},$$

where ${}^\circ T_{C_{\text{Ni}}}$ is the Curie temperature of nickel; ${}^\circ\beta_{\text{Ni}}$ is the magnetic moment of nickel; $T_{C_{\text{Cu-Ni}}}^{(\text{Cu, Ni}), i}$ and $\beta_{\text{Cu-Ni}}^{(\text{Cu, Ni}), i}$ are parameters calculated in [40]: $T_{C_{\text{Cu-Ni}}}^{(\text{Cu, Ni}), 0} = -935.5$; $T_{C_{\text{Cu-Ni}}}^{(\text{Cu, Ni}), 1} = -594.9$; $\beta_{\text{Cu-Ni}}^{(\text{Cu, Ni}), 0} = -0.7316$; $\beta_{\text{Cu-Ni}}^{(\text{Cu, Ni}), 1} = -0.3174$. The thermodynamic data on pure copper and nickel were taken from the SGTE database [44].

System Optimization. The model parameters A_i and B_i were optimized with the Thermo-Calc software. The phase diagram of the system is relatively simple and, therefore, most of the above experimental data could be accepted in the first stage of calculations for optimization: on phase equilibria [2–5]; thermodynamic properties of melts [4, 14, 15, 17–21, 23–25]; thermodynamic properties of hard alloys [27, 29–35]. The data [16, 28] on the formation enthalpies of liquid and solid alloys, respectively, were not included in the optimization. The data [25] on the thermodynamic activity of copper were accepted for optimization with smaller weight. At the first stage of calculations, thermodynamic models were restricted to only zero-order coefficients. At the next stage, the description of the thermodynamic properties of the (Cu, Ni) phase (the accuracy in describing the solidus and liquidus lines being retained) could be improved by keeping the first-order coefficients in the relevant model.

Table 1 summarizes the model coefficients. They were used to calculate the phase boundaries and thermodynamic properties of liquid and solid copper–nickel alloys, which are shown with solid lines in Figs. 1–7.

TABLE 1. Model Parameters of Excessive Gibbs Free Energy (J/mole) of Copper–Nickel Phases

$\Delta G^{(\varphi), \text{ex}} = (1 - x_{\text{Ni}})x_{\text{Ni}}\sum_{i=0}^{n}(1 - 2x_{\text{Ni}})^i (A_i + B_i T)$		
i	A_i	B_i
	L	
0	14259	0.45
	(Cu, Ni)	
0	6877.12	4.6
1	−2450.1	1.87

CALCULATION RESULTS AND DISCUSSION

Figures 1 and 2 show that the liquidus and solidus lines are adequately described in this study. Only in the center of the phase diagram does our liquidus line pass approximately 10 K higher than the data [3, 4], which studied this phase boundary with a thermal analysis.

The best compliance of the mixing enthalpy of liquid alloys is observed with the data from calorimetric studies [17, 21]. Based on calculations, the maximum value of the function is $\Delta H_{max} = 3.6$ kJ/mole. The activities of the components are best described for the data [26]. The maximum excess free mixing energy of melts at 1753 K is $\Delta G_{max}^{ex} = 3.8$ kJ/mole for the model. The extreme values of these two thermodynamic functions are close and thus the configuration contribution to the entropy is close to zero. According to the thermodynamic model, the supercooled melts may undergo immiscibility. The critical temperature of this metastable process is 882 K and, therefore, the melt is supercooled by more than 700 K relative to the liquidus temperature.

The curve of the integral mixing enthalpy of the (Cu, Ni) phase demonstrates the best agreement with [30] for copper-rich alloys and with [29] for nickel-rich alloys. The maximum of the function is $\Delta H_{max} = 1.8$ kJ/mole at $x_{Ni} = 0.58$. The resulting isotherm a_{Ni}^{1273} satisfactory presents the most reliable data on the thermodynamic properties of hard alloys — a set of values from [32, 33, 35]. The model correctly represents the temperature dependence of the thermodynamic activity of nickel established in [32]. The calculation of a_{Cu}^{1000} agrees with the data [31] for alloys with $x_{Ni} = 0$–0.7. The excess free mixing energy of solid solution components at 1000 K reaches its maximum $\Delta G_{max}^{ex} = 2.9$ kJ/mole near the equiatomic composition. The minimum excess mixing entropy is $\Delta S_{min}^{ex} = -1.2$ J/(mole · K) at $x_{Ni} = 0.4$.

The thermodynamic model of the (Cu, Ni) phase was used to calculate the miscibility gap. Figure 3 shows that the calculated bimodal $T_{bin}^{(Cu, Ni)}$ agrees with most experimental data. The critical point is shifted toward nickel and has coordinates such as $T_{cr} = 605$ K and $x_{Ni} = 0.6$. The binodal bends at the point intersecting the line of magnetic transformation in the (Cu, Ni) phase, which is evidence of the substantial magnetic contribution to free energy. Figure 3 shows the spinodal $T_{spin}^{(Cu, Ni)}$ of the (Cu, Ni) phase.

Therefore, the thermodynamic description of the system can represent the entire range of the thermodynamic properties of its phases and phase transformations, including low-temperature immiscibility of the solid solution. The excess thermodynamic mixing functions of liquid alloys are characterized by symmetric concentration dependence relative to the equiatomic composition. The maximum interaction in the (Cu, Ni) phase is observed in the region of nickel-rich alloys.

REFERENCES

1. M. Hansen and K. Anderko, *Constitution of Binary Alloys*, McGraw Hill, New York (1958).
2. B. D. Bastow and D. H. Kirkwood, "Solid/liquid equilibrium in the Copper–Nickel–Tin system determined by microprobe analysis," *J. Inst. Metals*, **99**, No. 9, 277–283 (1971).
3. E. A. Feest and R. D. Doherty, "The Cu–Ni equilibrium phase diagram," *J. Inst. Metals*, No. 3, 102–103.
4. B. Predel and R. Mohs, "Thermodynamische Untersuchung flussiger Nickel–Kupfer Legierungen," *Arch Eisenhut*, **42**, No. 8, 575–579 (1971).
5. E. Schurmann and E. Schultz, "Untersuchengen zum Verlauf der Liquidus und Solidus linien in den Systemen Kupfer–Mangan und Kupfer–Nickel," *Z. Metallkd.*, **62**, No. 10, 758–762 (1971).
6. F. A. Shunk (ed.), *Constitution of Binary Alloys*, McGraw-Hill, New York (1969).
7. D. J. Chakrabarti, D. E. Laughlin, S. W. Chen, et al., "Cu–Ni (copper–nickel)," in: *Phase Diagrams of Binary Copper Alloys*, ASM International, Ohio, OH (1994), pp. 276–286.
8. B. Mozer, D. T. Keating, and S. C. Moss, "Neutron measurement of clustering in the alloy CuNi [copper–nickel]," *Physical Review*, **175**, No. 3, 868–876 (1968).

9. M. F. Ebel, "X-ray measurements on spinodal decomposition in copper–nickel alloys," *Physica Status Solidi A*, **5**, No. 1, 91–94 (1971).

10. J. Vrijen and Radelaar, "Clustering in copper–nickel alloys: a diffuse neutron-scattering studyd," *Physical Review B*, **17**, No. 2, 409–421 (1978).

11. W. Wagner, R. Poerschke, A. Axmann, et al., "Neutron-scattering studies on an electron-irradiated (nickel-62)–41.4 at.% (copper-65) alloy," *Physical Review B*, **21**, No. 8, 3087–3099 (1980).

12. T. Tsakalakos, "Spinodal decomposition in copper–nickel alloys by artificial composition modulation technique," *Scripta Metallurgica*, **15**, No. 3, 255–258 (1981).

13. R. E. Pawel and E. E. Stansbury, "The specific heat copper, nickel and copper–nickel alloys," *J. Phys. Chem. Sol.*, **26**, No. 3, 607–613 (1965).

14. M. G. Benz and J. F. Elliott, *High Temperature Heats of Mixing for the Liquid Copper–Tin System and the Liquid Copper–Nickel System*, U.S. At. Energy Comm., **NYO-4691**, 1963, p. 36.

15. R. N. Dokken and J. F. Elliott, "Calorimetry at 1100°C to 1200°C: The copper–nickel, copper–silver, copper–cobalt systems," *Trans. Metal. Soc. AIME*, **233,** 1351–1358 (1965).

16. Abu El Hasan, Abdelazis, and A. A. Vertman, "Thermal chemistry of iron- and nickel-based melts," *Izv. AN SSSR. Metally*, No. 3, 19–30 (1966).

17. Y. Tozaki, Y. Iguchi, Ban-ya-Shiro, et al., "Heat of mixing of iron alloys," in: *Int. Symp. Met. Chemistry: Appl. Ferrous Met.* (July 19–21, 1971), Shaffield (1971), pp. 130–132.

18. Y. Iguchi, Y. Tozaki, M. Kakizaki, et al., "Calorimetric examination of mixing heats of nickel and cobalt alloys," *J. Iron and Steel Inst. Jap.*, **63,** 953–961 (1977).

19. S. Sato and O. J. Kleppa, "Enthalpies of formation of borides of iron, cobalt and nickel by solution calorimetry in liquid copper," *Metal. Trans.*, **B13**, 251–257 (1982).

20. U. K. Stolz, I. Arpshofen, F. Sommer, et al., "Determination of the enthalpy of mixing of liquid alloys using a high-temperature mixing calorimeter," *J. Phase Equilibria*, **14**, No. 4, 473–478 (1993).

21. M. A. Turchanin, S. V. Porokhnya, L. V. Belevtsov, et al., "Thermodynamic properties of liquid copper–nickel alloys," *Rasplavy*, No. 4, 8–12 (1994).

22. H. O. Samson–Himmelstjerna, "Heat content and heat of formation of molten alloys," *Z. Metallkd.*, **28**, No. 7, 197–202 (1936).

23. C. W. Schultz, G. R. Zellars, S. L. Payne, et al., "Activities of copper and nickel in liquid copper–nickel alloys," *Bureau of Mines Report of Investigations*, **6410**, No. 4, 9 (1964).

24. A. D. Kulkarni and R. E. Johnson, "Thermodynamic studies of liquid copper alloys by electromotive force method. II. Copper–nickel–oxygen and copper–nickel systems," *Metal. Trans.*, **4**, No. 7, 1723–1727 (1973).

25. V. V. Berezutskii and G. M. Lukashenko, "Thermodynamic properties of liquid nickel–copper alloys," *Ukr. Khim. Zh.*, No. 10, 1029–1032 (1987).

26. J. Tomiska and A. Neckel, "Knudsen-cell mass spectrometry for the determination of the thermodynamic properties of liquid copper–nickel alloys," *Int. J. Mass Spectrometry and Ion Physic,* **47,** 223–226 (1983).

27. O. Kubaschewski, W. A. Dench, and V. A. Genta, "A High temperature calorimeter for slow reactions," in: *The Physical Chemistry of Metallic Solutions and Intermetallic Compounds*, Vol. 1, His Majesty's Stationery Office, London (1958), pp. 1–8.

28. J. S. L. Leach and M. B. Bever, "On the heats of formation of copper–nickel alloys," *Trans. Met. Soc. AIME*, **215**, No. 4, 728–729 (1959 (1960)).

29. R. J. Oriani and U. K. Murphy, "Heats of formation of solid nickel–copper and nickel–gold alloys," *Acta Met.*, **8,** 23–25 (1960).

30. L. Elford, F. Muller, and O. Kubaschewski, "Thermodynamic properties of copper–nickel alloys," *Ber. Bunsengesellschaft*, **73,** 601–605 (1968).

31. A. A. Vecher and Ya. I. Gerasimov, "Studying the thermodynamic properties of binary metal systems with the emf method. VIII. Solid copper–nickel solutions," *Zh. Fiz. Khim.*, **37**, No. 3, 490–498 (1963).

32. R. A. Rapp and F. Maak, "Thermodynamic properties of solid copper–nickel alloys," *Acta Metallurgica*, **10**, No. 1, 63–69 (1962).

33. A. Kontopoulos, "Thermodynamic activities in copper–nickel–iron solid solutions," *Praktika tes Akademias Athenon*, **52**, No. A–D, B607–B619 (1978).

34. J. C. Gachon, M. Notin, C. Cunat, et al., "Enthalpy of formation and excess entropy for dulite copper-based alloys: experimental and theoretical study," *Acta Metallurgica*, **28**, 489–497 (1980).

35. Z. Moser, W. Zakulski, P. Spencer, et al., "Thermodynamic investigations of solid Cu–Ni and Fe–Ni alloys and calculation of the solid state miscibility gap in the Cu–Fe–Ni system," *CALPHAD*, **9**, No. 3, 257–269 (1985).

36. Ya. I. Gerasimov, A. A. Vecher, and V. A. Geiderikh, "Thermodynamic properties of solid copper–nickel and iron–cobalt solutions," *Dokl. AN SSSR*, **122**, 834–836 (1958).

37. I. Katayama, H. Shimatani, and Z. Kozuka, "Thermodynamic study of solid Cu–Ni and Ni–Mo alloys by E.M.F. measurements using solid electrolyte," *J. Jap. Inst. Met.*, **37**, No. 5, 509–515 (1973).

38. L. Kaufman, "Coupled phase diagrams and thermochemical data for transition metal binary systems. III," *CALPHAD*, **2**, No. 2, 117–146 (1978).

39. R. C. Sharma, "Thermodynamic Analysis of Cu–Ni System," *Trans. Indian Inst. Met.*, **35,** 372–375 (1982).

40. A. A. Jansson, *Thermodynamic Evaluation of the Cu−Fe−Ni System*, Trita-mac 0340, Royal Institute of Technology, Stockholm (1987), pp. 1–10.

41. G. Inden, "Determination of chemical and magnetic interchange energies in bcc alloys. III. Application to ferromagnetic alloys," *Z. Metallkd.*, **68**, 529–534 (1977).

42. M. Hillert and M. Jarl, "A model for alloying effects in ferromagnetic metals," *CALPHAD*, **2**, 227–238 (1978).

43. J.–O. Andersson, T. Helander, L. Hoglund. et al., "Thermo-Calc & DICTRA, computational tools for materials science," *CALPHAD*, **26**, No. 2, 273–313 (2003).

44. A. T. Dinsdale, "SGTE data for pure elements," *CALPHAD*, **15**, 317–425 (1991).